



ELSEVIER

Journal of Chromatography A, 732 (1996) 377–384

JOURNAL OF
CHROMATOGRAPHY A

Characterization and separation of inorganic fine particles by capillary electrophoresis with an indifferent electrolyte system

C. Quang¹, S.L. Petersen, G.R. Ducatte, N.E. Ballou*

Chemical Sciences Department, Pacific Northwest Laboratory, P.O. Box 999, MS P7-07, Richland, WA 99352, USA

Received 29 May 1995; revised 31 October 1995; accepted 9 November 1995

Abstract

The feasibility of using capillary electrophoresis to characterize and separate submicrometer- and micrometer-size metal oxide particles (e.g., TiO_2 , Al_2O_3 , and Fe_2O_3) was investigated. The use of indifferent electrolyte solutions such as sodium nitrate solutions leads to an electrolyte system without specific surface adsorption of ions but with essentially only electrostatic interactions between electrolyte ions and the surface of metal oxide particles. This system permitted development of a two-site dissociation model that was then applied to a description of the electrophoretic mobility of metal oxide particles as a function of the pH of the indifferent electrolyte solution. The use of unbuffered solutions, along with the tendency of metal oxide particles to form aggregates, prohibits the accurate determination of the electrophoretic mobility. Therefore, only a general agreement between the predicted electrophoretic mobilities and the measured values was obtained using the model. Also, general agreement was achieved between the estimated isoelectric points for the metal oxides and the values reported in the literature. Furthermore, the optimum conditions for separating mixtures of metal oxide particles in indifferent electrolyte solutions were identified. Successful separations of different kinds of metal oxide particles and of metal oxide particles with different polymorphic forms were achieved.

Keywords: Particles, inorganic; Metal oxides

1. Introduction

In the last decade there has been a major increase in the use of capillary electrophoresis (CE) for separating substances ranging from pharmaceutical compounds to large biomolecules [1,2]. Electrophoretic techniques are not limited to soluble molecules, but also can be used for the separation and characterization of particulate materials. This was demonstrated in the pioneering work of Hjertén in the

1970s using viral particles and bacterial particles [3]. The uniqueness of using CE for the separation and characterization of particles has also been shown in the recent work of VanOrman and McIntire [4–6], McCormick [7], and in work from this laboratory [8–10].

This paper describes the application of automated CE for separation of inorganic fine particles. Relatively few reports have dealt with the separation and characterization of inorganic fine particles by CE [7,10] even though there is a long history of studies of interfacial properties of inorganic fine particles by electrophoresis [11,12].

Because of the importance of inorganic fine

*Corresponding author.

¹ Present address: Olin Research Center, 350 Knotter Drive, P.O. Box 586, Cheshire, CT 06410-0586, USA.

particles to important industrial, environmental, medical and academic problems, increasing attention has been given to studies of the interfacial properties of such particles and to acquiring information on their particle size (or size distribution) and surface characteristics [13–17]. Measurement of the electrophoretic mobility (μ_{ep}) of metal oxide particles plays an essential role in analyzing the interfacial properties of the particles. This is due to the fact that the zeta potential (ζ) of the particles is related to the electrophoretic mobility by the well-known Smoluchowski equation:

$$\mu_{ep} = \frac{\epsilon\zeta}{4\pi\eta} E \quad (1)$$

where ϵ and η are the dielectric constant and coefficient of viscosity of the fluid, respectively, and E is the applied electric field. The surface charge density can be estimated using the Gouy–Chapman theory of the electrical double layer or other more sophisticated models [17].

The objectives of this work were to: (a) establish the feasibility of using automated CE instrumentation to measure the electrophoretic mobility of inorganic fine particles, and to estimate interfacial properties (e.g., isoelectric points, surface dissociation constants) of metal oxide particles; and (b) establish optimum conditions for separating mixtures of metal oxide particles by CE.

2. Experimental

2.1. Apparatus

The CE experiments were carried out on a Beckman P/ACE 2000 system. Fused-silica capillaries with 96 μm I.D. and 355 μm O.D. (Polymicro Technologies, Phoenix, AZ, USA) were used as separation columns. The total capillary length was 37.0 cm and the effective capillary length (the length to the detector) was 29.4 cm. The applied electric field was 300 V/cm. The capillary temperature was maintained at $25.0 \pm 0.1^\circ\text{C}$, and detection was conducted at the wavelength of 254 nm.

2.2. Reagents and chemicals

Indifferent electrolyte solutions with a constant ionic strength of 5.0 mM at various pH values were

prepared from double distilled nitric acid (Vycor, Columbus, OH, USA), reagent-grade sodium hydroxide (Aldrich, Milwaukee, WI, USA) and NANO-pure deionized water (Barnstead, Dubuque, IA, USA) (see Appendix for electrolyte solution calculation). Metal oxide powders were obtained from various sources (Table 1).

2.3. Procedures

Standard particle suspensions (ca. 100 ppm) were prepared by diluting stock particle suspensions that were prepared in deionized water with indifferent electrolyte solutions. The particle suspensions were mixed on a Vortex mixer and ultrasonicated for 5 min to enhance dispersion before being injected into the separation capillary. Injections were made for 2.0 s at ca. 0.5 p.s.i. (1 p.s.i. = 6894.76 Pa). The separation capillary was rinsed for 2 min with the corresponding electrolyte solution between runs. A solution of 0.5% (v/v) acetone in indifferent electrolyte solution was used to determine the electroosmotic flow. With the use of an indifferent electrolyte such as sodium nitrate, it was observed that the migration times of particle samples and the neutral marker changed significantly over time, especially at acidic and neutral pH conditions. This was presumably caused by aggregation of the metal oxide particles and by the lack of buffering capability, the slow equilibration of the metal oxide surfaces, and the irreproducibility of the capillary surface under the indifferent electrolyte conditions. It was found that reproducibility of electrophoretic mobility could be kept less than 5% relative standard deviation (R.S.D.) by frequently changing to fresh electrolyte solution (e.g., after three or four runs) and by determining the electroosmotic flow immediately after the sample run. The electrophoretic mobility

Table 1
Information on metal oxide powders

ID	Metal oxide	Source ^a	Size (μm)	Form
1	Al_2O_3	Johnson–Matthey	0.01	γ
2	Al_2O_3	Johnson–Matthey	0.3	γ, α
3	TiO_2	Polysciences	0.45	Rutile
4	Fe_2O_3	Polysciences	0.3–0.8	
5	Fe_3O_4	Polysciences	1.0	

^a Johnson–Matthey Electronics, Ward Hill, MA, USA and Polysciences, Warrington, PA, USA.

was calculated according to:

$$\mu_{ep} = \left(\frac{1}{t_m} - \frac{1}{t_{eo}} \right) \left(\frac{L_d}{E} \right) \quad (2)$$

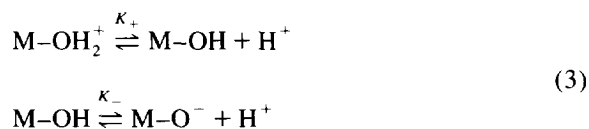
where t_m and t_{eo} are the migration times of sample particles and neutral marker, respectively, L_d is the capillary length to the detector, and E is the applied electric field strength.

Non-linear regression of the proposed model was carried out using SigmaPlot software (Jandel Scientific, Corte Madera, CA, USA).

3. Results and discussions

3.1. Theoretical background

Although they are quite different in chemical nature, metal oxides and proteins can be compared in respect to their surface charge behavior. The interfacial properties of both are dominated by the effect of pH and are influenced to a lesser extent by the ionic strength or salt concentration. In aqueous suspensions, a metal oxide particle can be treated as a diprotic acid [18]. The surface of such particles is positively charged at low pH where the first reaction of Eq. 3 predominates, and is negatively charged at high pH where the second reaction takes over.



The isoelectric point (pI) is the point at which the ζ potential is zero. At the pI , adsorption of cations is counterbalanced by the adsorption of anions and no electrokinetic phenomena are observed. In an indifferent (inert) electrolyte solution such as sodium nitrate solution, simple alkali metal ions and nitrate ions are attracted to charged surfaces by electrostatic forces. Under the above conditions the simple reactions of Eq. 3 apply and we have the following expressions for the acid dissociation constants:

$$\begin{aligned} K_+ &= \frac{[\text{M-OH}][\text{H}^+]}{[\text{M-OH}_2^+]} \\ K_- &= \frac{[\text{M-O}^-][\text{H}^+]}{[\text{M-OH}]} \end{aligned} \quad (4)$$

Similar to the treatment of ionizable solutes in CE [19,20], the electrophoretic mobility of metal oxide particles can be expressed as the weighted sum of two extreme mobilities (μ_+ , μ_-):

$$\mu_{ep} = F_+ \mu_+ + F_- \mu_- \quad (5)$$

where F values represent the molar fractions corresponding to positive or negative forms. For example,

$$\begin{aligned} F_+ &= \frac{[\text{M-OH}_2^+]}{[\text{M-OH}_2^+] + [\text{M-OH}] + [\text{M-O}^-]} \\ &= \frac{1}{1 + K_+ / [\text{H}^+] + K_+ K_- / [\text{H}^+]^2} \end{aligned} \quad (6)$$

Similarly, the expression for F_- in Eq. 5 can also be derived, and is as follows:

$$F_- = \frac{K_+ K_- / [\text{H}^+]^2}{1 + K_+ / [\text{H}^+] + K_+ K_- / [\text{H}^+]^2} \quad (7)$$

Substituting these expressions into Eq. 5, we obtain:

$$\mu_{ep} = \frac{\mu_+ + \mu_- K_+ K_- / [\text{H}^+]^2}{1 + K_+ / [\text{H}^+] + K_+ K_- / [\text{H}^+]^2} \quad (8)$$

This equation expresses the electrophoretic mobility of metal oxide particles μ_{ep} as a function of pH and parameters (μ_+ , μ_- , K_+ , K_-). The pH of electrolyte solutions is an experimentally controllable factor, and parameters can be estimated from the fitting of the above non-linear model to the experimental data. Then the electrophoretic mobility can be predicted at any pH within the defined pH range. Furthermore, the pI for oxide particles can be estimated by rearranging Eq. 8:

$$\text{pH}_{\mu_{ep}=0} = \frac{-\log(-K_+ K_- \mu_- / \mu_+)}{2} \quad (9)$$

3.2. Effect of pH on electrophoretic mobility

Measurements of the electrophoretic mobility of metal oxide particles (e.g., TiO_2 , Al_2O_3 , and Fe_2O_3) were carried out in 5.0 mM sodium nitrate solutions at various pH values. The practical pH range 3–12 was established because of the electric current limitation, that is, the high concentration of H^+ or OH^- ions outside this pH range leads to high electric

currents due to the high conductivity of H^+ and OH^- ions. At the applied electric field strength of 300 V/cm, the currents in most of the defined pH range remained almost constant at 12 μA , except at pH 3, 11.5, and 12 at which the electric currents were 22 μA , 30 μA , and 50 μA , respectively. The electrolyte solution of pH 12.0 was made of 10 mM sodium hydroxide solution.

Fig. 1 and Fig. 2 show the behavior of the electrophoretic mobility of four metal oxide particles. The electrophoretic mobility was positive at low pH conditions as expected when the first reaction of Eq. 3 predominates, and became negative at high pH values when the second reaction of Eq. 3 takes over. In an attempt to mathematically describe the data in Fig. 1 and Fig. 2, different kinds of model equations including an empirical model, a one-site dissociation model, and a two-site dissociation model, were tested for fitting the data of the electrophoretic mobility as a function of the pH. The model that worked best, as judged from the goodness-of-fit criterion of relative standard deviation (R.S.D.), was the two-site dissociation model described earlier in

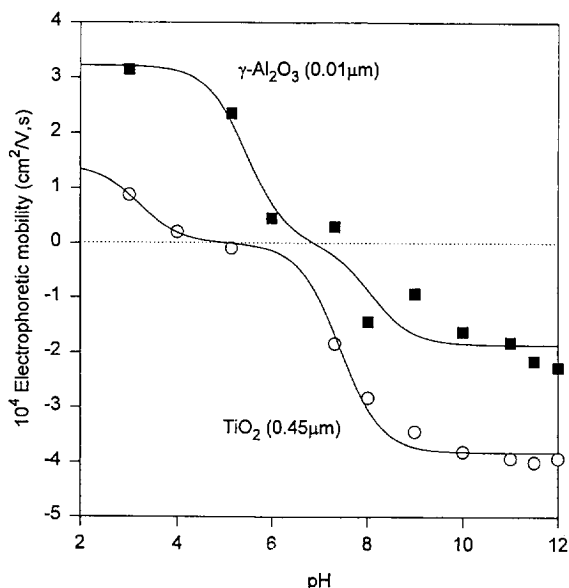


Fig. 1. Electrophoretic mobility of metal oxide particles ($\gamma\text{-Al}_2\text{O}_3$ and TiO_2) as a function of pH. Electrolyte: sodium nitrate solutions with a constant ionic strength of 5.0 mM. Symbols and solid lines represent the measured electrophoretic mobilities and theoretical best-fits, respectively.

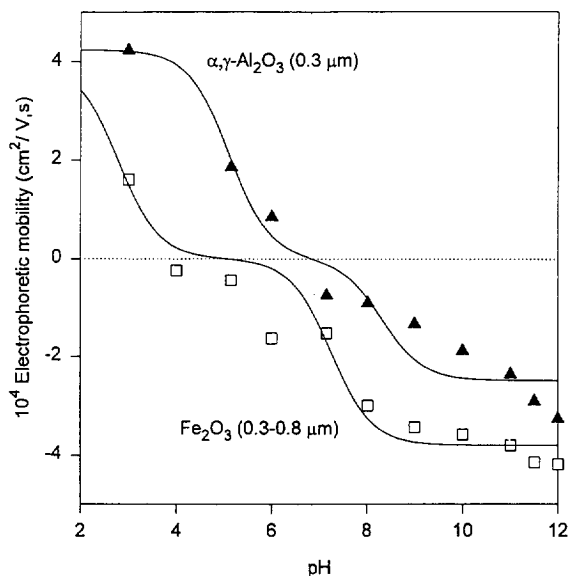


Fig. 2. Electrophoretic mobility of metal oxide particles ($\alpha,\gamma\text{-Al}_2\text{O}_3$ and Fe_2O_3) as a function of pH. Conditions as in Fig. 1.

this paper. With the two-site dissociation model, extreme mobilities (μ_+ , μ_-) and dissociation constants (K_+ , K_-) were estimated from fitting the proposed model (Eq. 8) to the experimental data. Subsequently, the pI for each metal oxide particles was estimated using Eq. 9. The results of regression analysis are summarized in Table 2.

As indicated by the data in Table 2, large values of R.S.D. were obtained for model parameters such as μ_+ and K_+ , especially for TiO_2 and Fe_2O_3 , which have pI values in the low pH range. This is probably due to the limitation of the electrophoretic mobility data at very low pH (i.e., $pH < 3$). Parameters of μ_+ and K_+ are strongly dependent on each other and show particularly large variations. Of course, best-fit parameters with R.S.D.s larger than 100% are meaningless. Although unbuffered electrolytes were used and there are difficulties in particle electrophoresis [3], a general agreement was nevertheless achieved between the predictions based on the proposed model and the measured results. The pI for TiO_2 (rutile) occurred at pH 5.0, which was the same as values reported in the literature [14,21]. The pI values for Fe_2O_3 , $\gamma\text{-Al}_2\text{O}_3$, and $\alpha,\gamma\text{-Al}_2\text{O}_3$ were also in general agreement with the reported values [22]. Note that the surface properties of these materials are known to

Table 2
Regression analysis results from fitting Eq. 8

Oxide		Value ^a	R.S.D. (%)	Dependence ^b	pI ^c
TiO ₂	μ_+	$1.44 \cdot 10^{-4}$	82	0.946	5.0
	μ_-	$-3.82 \cdot 10^{-4}$	2.2	0.131	
	K_+	$6.40 \cdot 10^{-4}$	192	0.946	
	K_-	$3.74 \cdot 10^{-8}$	20	0.131	
γ -Al ₂ O ₃	μ_+	$3.23 \cdot 10^{-4}$	15	0.308	6.9
	μ_-	$-1.85 \cdot 10^{-4}$	13	0.096	
	K_+	$3.40 \cdot 10^{-6}$	67	0.311	
	K_-	$8.54 \cdot 10^{-9}$	144	0.099	
Fe ₂ O ₃	μ_+	$4.00 \cdot 10^{-4}$	581	0.995	5.0
	μ_-	$-3.80 \cdot 10^{-4}$	7.4	0.115	
	K_+	$1.68 \cdot 10^{-3}$	914	0.995	
	K_-	$5.76 \cdot 10^{-8}$	7.02	0.115	
α,γ -Al ₂ O ₃	μ_-	$4.25 \cdot 10^{-4}$	14	0.21	6.8
	μ_+	$-2.49 \cdot 10^{-4}$	12	0.088	
	K_+	$7.98 \cdot 10^{-6}$	59	0.21	
	K_-	$4.87 \cdot 10^{-9}$	17	0.089	

^a Electrophoretic mobility units: cm²/V s.

^b The dependence of a parameter is defined to be dependence = 1 - (variance of the parameter, other parameters constants)/(variance of the parameter, other parameters changing). Parameters with dependencies near 1 are strongly dependent on one another (see SigmaPlot for Windows Manual).

^c Calculated values using Eq. 9.

depend on the method of preparation and sample treatment [22].

Fig. 3 shows electropherograms of TiO₂ particles under different pH conditions. At pH 10.0, TiO₂ particles were well dispersed, resulting in a larger and smoother peak than at low pH. In particular, at pH 4.0 the TiO₂ peak was relatively small and had numerous spikes. Solutions with a pH close to the pI of metal oxide particles are undesirable for stabilizing such particles because the particles derive their kinetic stability with respect to aggregation from inter-particle electrostatic repulsion. Particle aggregation and sedimentation were thought to be the cause of spiky peaks and less material being injected from the top of the injection vial. We note that particle peaks were generally much broader than those of 'point charge' molecules. This is probably caused by heterogeneity of the ζ potential on particles [17]. A detailed description on the zone broadening of particle peaks has been previously presented [9].

Predictions based on the difference of the observed electrophoretic mobilities indicated that pH 9.0 (5.0 mM sodium nitrate) would be satisfactory

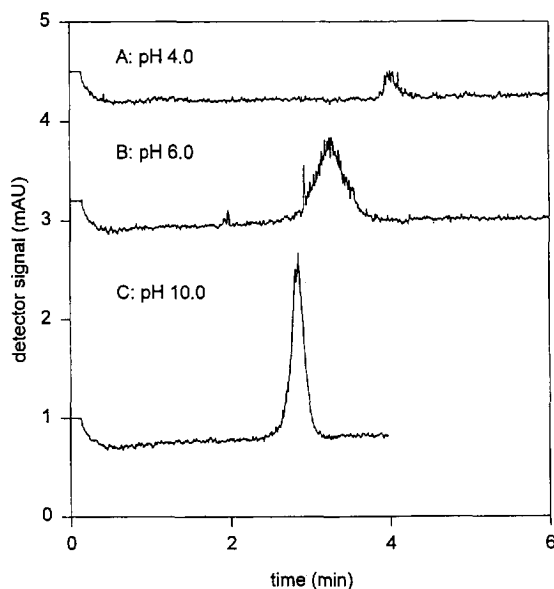


Fig. 3. Electropherograms of TiO₂ at different pH conditions. Electrolyte: sodium nitrate with a constant ionic strength of 5.0 mM.

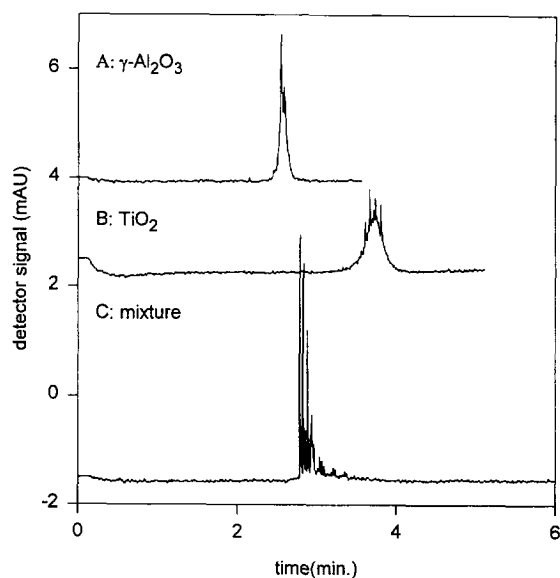


Fig. 4. Electropherograms at pH 9.0, 5.0 mM sodium nitrate.

for separating γ - Al_2O_3 and TiO_2 (see Fig. 1). However, as shown in Fig. 4C, a single peak with numerous spikes was obtained from the mixture of γ - Al_2O_3 and TiO_2 . This suggests that the mixed suspension of γ - Al_2O_3 and TiO_2 particles formed coaggregates and was not stable at this pH condition even though these two types of metal oxide particles form relatively stable suspensions separately (Fig. 4A and Fig. 4B).

Obviously, high pH solutions would provide better conditions for separating mixtures of metal oxide particles because most metal oxide particles become more negatively charged as pH increases, resulting in a stronger electrostatic repulsion and a kinetically more stable suspension for a metal oxide mixture. Fig. 5 shows the effect of pH on the separation of three kinds of metal oxide particles: γ - Al_2O_3 , α , γ - Al_2O_3 , and TiO_2 (rutile). It is possible to separate metal oxide particles on the basis not only of chemical identity, but also of polymorphic form. Fig. 6 gives more examples of the separation of metal oxide particles using a solution of 10 mM NaOH, pH 12.0.

3.3. Effect of ionic strength on particle separations

The ionic strength of the indifferent electrolyte solution is another factor that influences both the

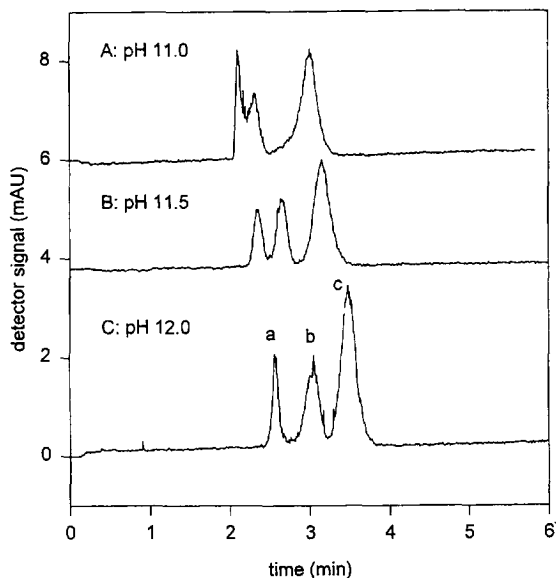


Fig. 5. Effect of pH on the separation of a mixture of α , γ - Al_2O_3 (a), γ - Al_2O_3 (b) and TiO_2 (c). Electrolyte: sodium nitrate with a constant ionic strength of 5.0 mM. The solution of pH 12.0 was made of 10 mM sodium hydroxide solution.

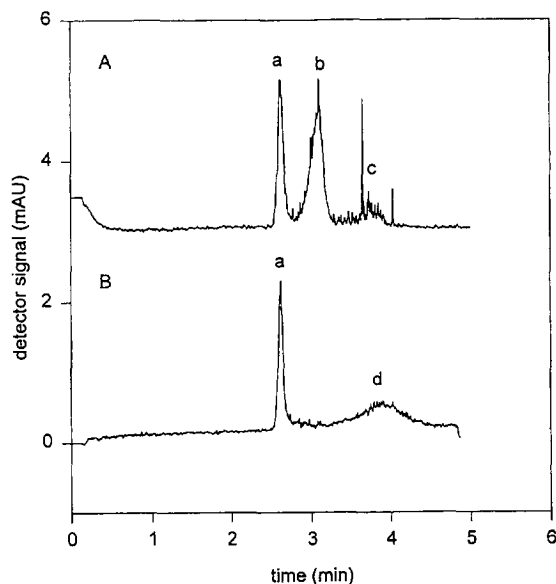


Fig. 6. Electropherograms of mixtures of α , γ - Al_2O_3 (a), γ - Al_2O_3 (b), Fe_3O_4 (c), and Fe_2O_3 (d) using the solution of 10 mM sodium hydroxide (pH 12.0).

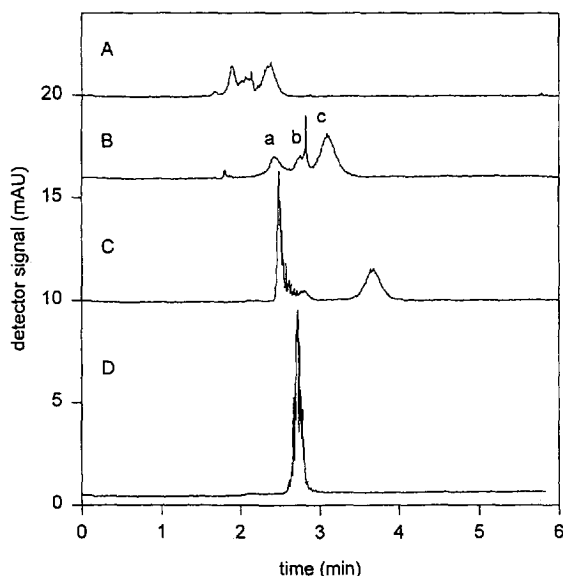


Fig. 7. Effect of ionic strength on the separation of a mixture of $\alpha,\gamma\text{-Al}_2\text{O}_3$ (a), $\gamma\text{-Al}_2\text{O}_3$ (b) and TiO_2 (c). Electrolyte: sodium nitrate at pH 11.0 with various ionic strengths as indicated in the figure. Ionic strengths: (A) 1.0 mM, (B) 2.5 mM, (C) 5.0 mM, (D) 10 mM.

electrophoretic behavior and stability of metal oxide particle suspensions. For another set of experiments, Fig. 7 shows the effect of ionic strength on the separation of the mixture of $\gamma\text{-Al}_2\text{O}_3$, $\alpha,\gamma\text{-Al}_2\text{O}_3$, and TiO_2 particles. The pH of the solutions was kept constant at 11.0 while changing the ionic strength. It is well understood that increasing ionic strength in a suspension of metal oxide particles causes the diffuse double layer of such particles to shrink. This increases the probability of particle interaction and aggregation. As shown in Fig. 7, lowering ionic strength generally results in a better suspension and a better separation of metal oxide particles. On the other hand, lowering ionic strength also leads to a stronger electroosmotic flow. This may actually decrease the separation resolution (R_s) as indicated by the following equation [23]:

$$R_s = \frac{\sqrt{N}}{4} \frac{\Delta\mu}{\mu_{av} + \mu_{eo}} \quad (10)$$

where N is the number of theoretical plates, $\Delta\mu$ and μ_{av} are the difference and average of the two electrophoretic mobilities, respectively, and μ_{eo} is the electroosmotic mobility. Note that the difference

in migration times of $\gamma\text{-Al}_2\text{O}_3$, $\alpha,\gamma\text{-Al}_2\text{O}_3$, and TiO_2 in 5.0 mM sodium nitrate and pH 11.0 solutions were observed in two experiments done about one month apart (Fig. 5 and Fig. 7). We believe that the changes in migration times mainly result from the irreproducibility of the electroosmotic flow, which is due to the variability of the surface of the fused-silica capillary, especially in an indifferent electrolyte system.

4. Conclusions

We have demonstrated the feasibility of using CE to characterize metal oxide particles in indifferent electrolyte solutions. A mathematical formulation based on a two-site dissociation model was proposed to describe the electrophoretic behavior of metal oxide particles as a function of pH. The extent of agreement was reasonably good considering the instability of suspensions of submicrometer- and micrometer-size metal oxide particles, the use of unbuffered electrolyte solutions, and the irreproducibility of the surface conditions of fused-silica capillary in unbuffered electrolyte solutions. The estimated pI values of metal oxide particles were in general agreement with the literature values.

In an indifferent electrolyte solution, metal oxide particles acquire a surface charge due to dissociation of acidic surface groups. As a consequence, solutions of high pH and low ionic strength provide relatively stable suspensions and generally better separations of mixtures of metal oxide particles. It may be possible to introduce various surface chemical modifications such as specific ion adsorption, cation exchange, and surfactant modification in order to manipulate separation selectivity and to study surface adsorption. Work is presently under way in this direction.

Acknowledgments

This work was supported by the U.S. Department of Energy. Pacific Northwest Laboratory is operated for the U.S. Department of Energy by Battelle Memorial Institute under Contract DE-AC06-76RLO 1830.

Appendix 1

Algorithm for the calculation of electrolyte compositions

The interfacial properties of metal oxide particles are critically dependent on the pH and ionic strength of the solution. For systematic study, it is often desirable to make measurement over a wide pH range, at the same time maintaining constant ionic strength in the medium. For this reason, the following algorithm was derived for the calculation of the electrolyte compositions for indifferent electrolyte solutions.

In an indifferent electrolyte solution such as sodium nitrate, the formal concentrations of nitric acid (C_a) and sodium hydroxide (C_b) are equal to the concentrations of NO_3^- and Na^+ , respectively:

$$C_a = [\text{NO}_3^-], \text{ and } C_b = [\text{Na}^+] \quad (\text{A1})$$

From the balance of charge, we have:

$$[\text{Na}^+] + [\text{H}^+] = [\text{OH}^-] + [\text{NO}_3^-] \quad (\text{A2})$$

From the definition of ionic strength, we have:

$$\text{Ionic strength} = 0.5 ([\text{Na}^+] + [\text{H}^+] + [\text{OH}^-] + [\text{NO}_3^-]) \quad (\text{A3})$$

Combining Eqs. A2 and A3 to eliminate $[\text{Na}^+]$ and $[\text{H}^+]$ leads to:

$$\text{Ionic strength} = [\text{OH}^-] + [\text{NO}_3^-] \quad (\text{A4})$$

Replacing $[\text{OH}^-]$ with $K_w/[\text{H}^+]$ and rearranging Eq. A4, we obtain:

$$[\text{NO}_3^-] = \text{ionic strength} - \frac{K_w}{[\text{H}^+]}$$

or:

$$C_a = \text{ionic strength} - \frac{K_w}{[\text{H}^+]} \quad (\text{A5})$$

From Eq. A2 we have:

$$C_b = \text{ionic strength} - [\text{H}^+] \quad (\text{A6})$$

Given the pH and ionic strength of an indifferent electrolyte solution, the formal concentrations of nitric acid and sodium hydroxide (C_a , C_b) can be calculated from the above equations. The calculations can be easily done by using a spreadsheet such as Quattro-Pro or Excel.

References

- [1] W.G. Kuhr and C.A. Monnig, *Anal. Chem.*, 64 (1992) 389R.
- [2] C.A. Monnig and R.T. Kennedy, *Anal. Chem.*, 66 (1994) 314R.
- [3] S. Hjerten, in H. Bloemendal (Editor), *Cell Separation Methods*, Elsevier/North-Holland Biomedical Press, 1977, p. 119.
- [4] B.B. VanOrman and G.L. McIntire, *J. Microcol. Sep.*, 1 (1989) 289.
- [5] B.B. VanOrman and G.L. McIntire, *Am. Lab.*, November (1990) 66.
- [6] B.B. VanOrman-Huff and G.L. McIntire, *J. Microcol. Sep.*, 6 (1994) 591.
- [7] R.M. McCormick, *J. Liq. Chromatogr.*, 14 (1991) 939.
- [8] H.K. Jones and N.E. Ballou, *Anal. Chem.*, 62 (1990) 2484.
- [9] S.L. Petersen and N.E. Ballou, *Anal. Chem.*, 64 (1992) 1676.
- [10] S.L. Petersen and N.E. Ballou, *Pittsburgh Conference on Analytical Chemistry and Applied Spectroscopy*, New Orleans, LA, March 5–10, 1995, Abstract 311P.
- [11] R.J. Hunter, *Zeta Potential in Colloid Science*, Academic Press, London, 1981, Ch. 4.
- [12] R.J. Hunter, *Introduction to Modern Colloid Science*, Oxford Science Publications, Oxford, 1993, Ch. 8.
- [13] C. Boxall, *Chem. Soc. Rev.*, 23(2) (1994) 137.
- [14] C. Boxall and G.H. Kelsall, *J. Chem. Soc. Faraday Trans.*, 87 (1991) 3537.
- [15] C. Boxall and G.H. Kelsall, *J. Chem. Soc. Faraday Trans.*, 87 (1991) 3547.
- [16] S. Sugrue, *Am. Lab.*, April (1992) 64.
- [17] M.C. Fair and J.L. Anderson, *Langmuir*, 8 (1992) 2850.
- [18] C. Huang and W. Stumm, *J. Colloid Interface Sci.*, 43 (1973) 409.
- [19] J.P. Foley, *Anal. Chem.*, 62 (1990) 1302.
- [20] C. Quang, J.K. Strasters and M.G. Khaledi, *Anal. Chem.*, 66 (1994) 1646.
- [21] P. Tsai, C. Wu and C.S. Lee, *J. Chromatogr. B*, 657 (1994) 285.
- [22] G.A. Parks, *Chem. Rev.*, 65 (1965) 177.
- [23] J.W. Jorgenson and K.D. Lukacs, *Anal. Chem.*, 53 (1981) 1298.